Development of a Software for the Numerical Modeling of Reinforced Concrete Sections - AlfaMCV

Ana Waldila de Queiroz Ramiro Reis, Undergraduate Student[1], Margareth da Silva Magalhães, D.Sc.[2] and Rodrigo Bird Burgos, D.Sc.[3]

[1]Rio de Janeiro State University; e-mail: anawaldila@hotmail.com
[2]Department of Civil Construction and Transportation, Rio de Janeiro State University; e-mail: margareth.magalhaes@uerj.br
[3]Department of Structures and Foundations, Rio de Janeiro State University; e-mail: rburgos@eng.uerj.br

ABSTRACT

In the design of reinforced concrete structures, the usual procedure is the inclusion of safety factors, according to the Brazilian Standards, to allow the structure to withstand loads above the predicted and a possible collapse. Since concrete has greater resistance to compression than tension, the design of this type of structures disregards its contribution in terms of tensile forces. In this way, the present work aims to analyze the contribution of the tension region of the concrete when submitted to a bending moment. Finally, based on this mathematical model, a software is developed to represent the behavior of a beam (strains, curvature and deflections), according to the application of a resisting bending moment, until rupture.

Keywords: Bending, Moment, Mathematical, Model

1. Motion and Significance

Structural reinforced concrete is composed by a brittle material (concrete) and a ductile material (steel). In the design of structures of this nature, tensile stresses of the concrete are considered null, since they correspond to a small percentage of the compression stresses. These stresses vary according to the distance from a line, called neutral axis, along which stresses are effectively zero, as shown in Fig.1.1. This variation of the height of the neutral axis comes from the application of a resisting moment whose rupture occurs where the strains of the concrete reach 3.5 ‰ under flexo compression (PFEIL, 1969 [[14]; REIS, 2017 [[16]).

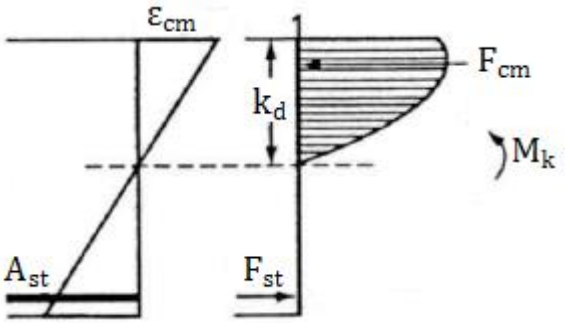

Fig. 1.1. Reinforced concrete section stress distribution (CHUST, 2007)

The analysis of the tensioned region performed by BAZANT (1984) [1] considers the classical model of stress variation, which is represented by a bilinear diagram, in which the tensile stress increases until the maximum tensile strength f_{tk} is reached, and then presenting a linear descent until reaching the maximum strain and zero stress (Fig.1.2.). In this linear descent, the section is undergoing the process of crack propagation, from the most to the least tensioned fibers, according to Fig.1.1. With the propagation of the same, the collaboration of the traction concrete becomes null and then the section collapses either by the crushing of the compressed concrete or by the rupturing of the pulling steel.

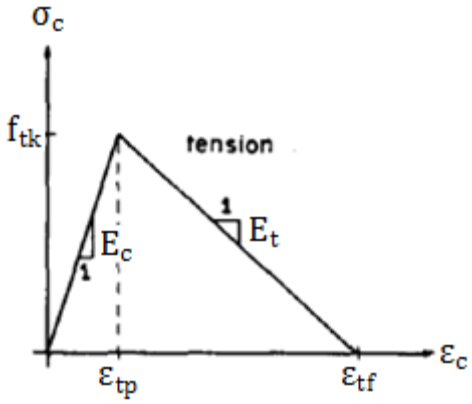

Fig. 1.2. Bilinear behavior of concrete in tension (BAZANT, 1984 [2])

In order to perform the modeling of the tensile part of concrete in the structure, it is necessary to analyze the propagation behavior of the cracks, according to fracture mechanics theory. In this way, the context becomes more complex for analysis. Based on this, AlfaMCV software was developed by REIS (2017) [[16], whose objective is the performance of reinforced concrete beams based on the versatility of the user input. Based on geometries of the beam structure, concrete and steel characteristics, the program calculates the slope of the structure and provides a table with information such as neutral line height, deformation of the materials, maximum moment in the beam and deflection caused by the applied load. These output data are based on the steady-state data of the structure, are analyzed as the base and split database of the concrete, as well as the material between the cracks, based on the fracture energy model. In addition, the end-of-knowledge diagram is normal according to SAENZ (1964) [[17], since it is polynomial (first and

second degree) to describe more accurately the behavior of concrete to compression. Already started, two linear equations delimit the strain - strain graph.

2. Concrete Stress – Strain BehaviorCONCRETE STRESS-STRAIN BEHAVIOR

The model studied by BAZANT (1984) [3] corresponds to a simply supported beam of rectangular section submitted to a point load in the middle of the span, that is, one of the possible representative laboratory tests. Thus, strains from creep and shrinkage of concrete are not considered since they required a longer period of time to appear.

Based on Fig.1.2., the representative equations, calculated by SCANLON (1971) [4] correspond to:

$$\varepsilon_c \leq \varepsilon_{tp} \rightarrow \sigma_c = E_c \varepsilon_c \quad (1)$$

$$\varepsilon_{tp} < \varepsilon_c < \varepsilon_{tf} \rightarrow \sigma_c = f_{tk} - (\varepsilon_c - \varepsilon_{tp})(-E_t) \quad (2)$$

$$\varepsilon_{tf} < \varepsilon_c \rightarrow \sigma_c = 0 \quad (3)$$

These equations represent, respectively, the regions shown in Fig.1.2., i. e., the increase of the stress until reaching the tensile strength of concrete, the descent due to cracking and the strains that cause null stress.

However, the description of the behavior of concrete is not completely described by the equations above. They should be complemented by the theory of fracture mechanics, adding concepts about concrete modulus of elasticity (E_c), tangent modulus (E_t) and fracture energy for the formation of cracks in the section. (VITTORIO, 2011[5])

3. Fracture Mechanics

The relation between the elastic moduli E_c and E_t of concrete is based on the theory of fracture mechanics, considering the concrete as a heterogeneous material that has discontinuities in the stresses that act in the section, originating from strains caused by micro cracking. (REIS, 2017 [[16])

In the theory of fracture mechanics applied to fragile materials, collapse occurs when the material reaches its maximum tensile stress, causing a sudden drop of local stresses. This fracture is only analyzed correctly when the absorbed energy is calculated. That is, it can be seen that the generation of cracks comes from a discontinuity of stresses in a certain infinitesimal element analyzed in the material.

However, it is important to point out that these concepts are applied to the concrete material alone. In the case of reinforced concrete structures, it is seen that even in its tension region and with an already cracked area, concrete between cracks is still capable of absorbing energy coming from the stresses to which it is submitted, since there is the collaboration of the steel reinforcement. (PROENÇA, 1988 [[15])

Based on these concepts, the beginning of concrete cracks occurs when the energy of application of the load on the beam is no longer totally absorbed by the concrete, originating a fissure. In this way, since concrete is a heterogeneous material, in its own microscopic structure there are places of greater and smaller strengths. The fissure naturally propagates through regions of lower strengths, until it generates a node in the material. Then, the formation of fractures in the concrete takes place, according to Fig.3.1.

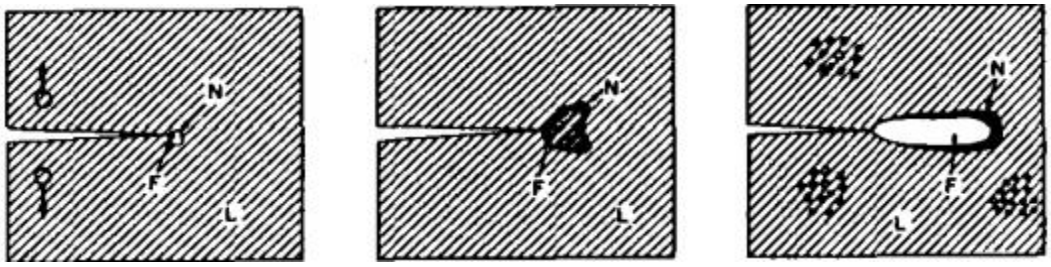

Fig. 3.1. Crack growth in concrete (BAZANT, 1983 [[13]])

Based on these concepts, it is possible to build a three-dimensional model of tensile-strain relationships, based on the concrete modulus of elasticity and the Poisson effect:

$$\begin{Bmatrix}\varepsilon_x\\ \varepsilon_y\\ \varepsilon_z\end{Bmatrix} = \frac{1}{E_c}\begin{bmatrix}1 & -\nu & -\nu\\ -\nu & 1 & -\nu\\ -\nu & -\nu & 1\end{bmatrix}\begin{Bmatrix}\sigma_x\\ \sigma_y\\ \sigma_z\end{Bmatrix} + \begin{bmatrix}0\\ 0\\ \varepsilon_f\end{bmatrix} \quad (4)$$

where ε_f is the average strain that originates the crack.

It is worth mentioning that for a practical analysis of the cracking process, it is valid to consider concrete as an elastic and isotropic material, in addition to assuming that the system consists of a dense and uniformly distributed concrete.

4. Concrete Fracture Energy

The process of loading a beam in a structural system involves the generation of energy. Part of this energy is absorbed by concrete and steel, another part is manifested as cracking. The energy that is manifested in cracks is called fracture energy and is determined by:

$$\mathcal{G}_f = \frac{w_c \cdot f_{tk}^2}{2C_f} \quad (5)$$

Such energy is directly related to the effective crack width w_c, tensile strength of the concrete used (f_{tk}) and the slope of the stress-strain curve, C_f.

In the case of the effective width, it is directly related to the maximum diameter of the large aggregate for the confection of the concrete. According to research carried out (BAZANT, 1983 **[**[13]**]**; BAZANT, 1985 [[12]]), it was observed that the relation between the width and the diameter of the aggregate corresponds to 3, as in:

$$w_c = 3d_a \quad (6)$$

In order to obtain a definite relation between E_c and E_t, research was carried out to correlate the tangent slope C_f with the tensile strength. Using data from several tests (BAZANT, 1983 **[**[13]**]**), it is possible to obtain a relation between C_f and f_{ck}, by fitting a curve that best represents this behavior:

$$C_f = 1{,}811 + 0{,}0143 f_{tk} \quad (7)$$

Finally, using the equations above, it is possible to obtain a relation between concrete elastic moduli E_c and E_t:

$$E_t = \frac{-69{,}9E_c}{56{,}7+f_{tk}} \quad (8)$$

5. Equation for Concrete Under Compression

Several numerical models have been developed to describe the behavior of concrete under compression. One of the most accepted models in the literature is the one developed by SAENZ (1964) [[17], in which a linear relation between stress and strain is divided by a 2nd degree polynomial. Fig.5.1. shows de physical meaning of all the parameters in the equation.

$$\sigma_c = \frac{E_c \cdot \varepsilon_c}{1+\left(\frac{E_c \cdot \varepsilon_{cp}}{f_{ck}}-2\right)\left(\frac{\varepsilon_c}{\varepsilon_{cp}}\right)+\left(\frac{\varepsilon_c}{\varepsilon_{cp}}\right)^2} \quad (9)$$

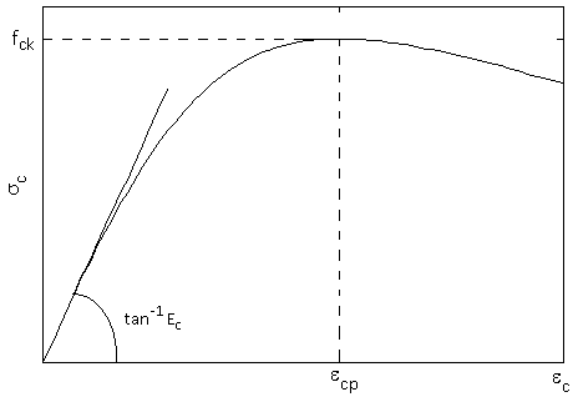

Fig. 5.1. Stress-strain relation for concrete under compression

6. Equilibrium Equations

In order to determine the resisting moment of the cross section, equilibrium is required in terms of forces and moments, as shown in Fig.6.1.:

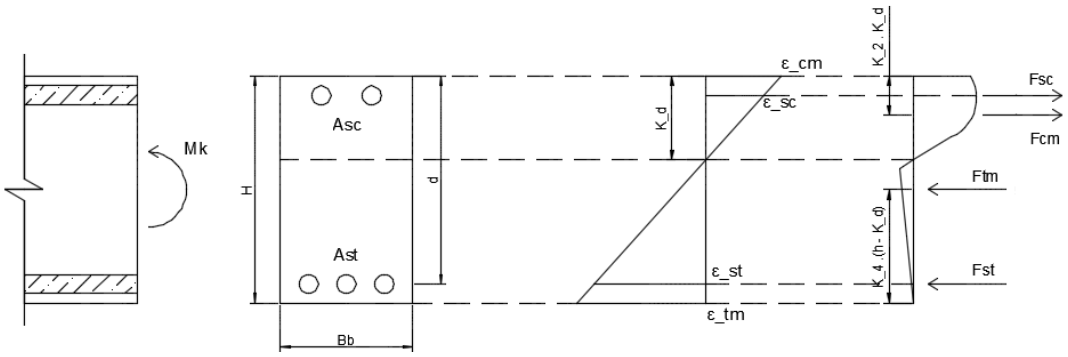

Fig. 6.1. (a) Reinforced concrete section; (b) Strain distribution; (c) Stress distribution (REIS, 2017 [[16]])

As shown in Fig.6.1., compressive (F_{cm}) and tensile (F_{tm}) forces in concrete are given by:

$$F_{cm} = k_1 \, f_{ck} \, b \, k_d \tag{10}$$

$$F_{tm} = k_3 \, f_{tk} \, b \, (h - \, k_d) \tag{11}$$

where k_1 and k_3 are the heights of equivalent rectangles for the compression and tension regions, respectively (BAZANT ,1984 [6]).

Thus, based on the equilibrium of the system of Fig.6.1., the height of the neutral axis is determined for a certain level of strain.

Finally, by obtaining the height of the neutral axis, it is possible to determine the resisting moment of the structure, based on the following relation:

$$M = \begin{bmatrix} k_1 . f_{ck} . B_b . k_d \left(\frac{H}{2} - k_2 k_d\right) + \left(\sum_{j=1}^{2} \sigma_{sj} . A_{sj}\right) \left(\frac{H}{2} - d_j\right) - \\ k_3 . f_{tk} . B_b . (H - k_d) \left(\frac{H}{2} - k_4 (H - k_d)\right) \end{bmatrix} \tag{12}$$

where k_2 and k_4 are the centroids of the resultant forces for the compression and tension regions, respectively.

For a certain level of strain, there is a value for k_1, k_2, k_3 and k_4, which are dependent on the values of compressive and tensile strains of concrete.

6.1.For $\varepsilon_c \leq \varepsilon_{tp} \rightarrow \sigma_c = E_c\varepsilon_c$

$$k_1 = \frac{E_c}{f_{tk}\cdot\varepsilon_{cm}}\left[\begin{array}{c}\frac{1}{2B}\ln(B{\varepsilon_{cm}}^2 + A\varepsilon_{cm} + 1) + \\ + \frac{A}{2B}\cdot\frac{2}{\sqrt{4B-A^2}}\cdot\left(arctg\left(\frac{A}{\sqrt{q}}\right) - arctg\left(\frac{2B\varepsilon_{cm}+A}{\sqrt{q}}\right)\right)\end{array}\right] \quad (13)$$

$$k_2 = 1 - \frac{\left[\begin{array}{c}\frac{\varepsilon_{cm}}{B} + \left(\frac{A^2-2B}{B^2\sqrt{q}}\right).arctg\left(\frac{2B\varepsilon_{cm}+A}{\sqrt{q}}\right) - \\ \frac{A}{2B^2}\ln(B\varepsilon_{cm}^2 + A\varepsilon_{cm}+1) - \left(\frac{A^2-2B}{B^2\sqrt{q}}\right).arctg\frac{A}{\sqrt{q}}\end{array}\right]}{\varepsilon_{cm}\left[\begin{array}{c}\frac{1}{2B}\ln(B{\varepsilon_{cm}}^2 + A\varepsilon_{cm}+1) + \\ + \frac{A}{2B}\cdot\frac{2}{\sqrt{4B-A^2}}\cdot\left(arctg\left(\frac{A}{\sqrt{q}}\right) - arctg\left(\frac{2B\varepsilon_{cm}+A}{\sqrt{q}}\right)\right)\end{array}\right]} \quad (14)$$

$$k_3 = \frac{E_c\cdot\varepsilon_{tm}}{2f_{tk}} \quad (15)$$

$$k_4 = \frac{1}{3} \quad (16)$$

6.2.For $\varepsilon_{tp} < \varepsilon_c < \varepsilon_{tf} \rightarrow \sigma_c = f_{tk} - (\varepsilon_c - \varepsilon_{tp})(-E_t)$

$$k_3 = \frac{1}{f_{tk}\,\varepsilon_{tm}}\left[\left(f_{tk} + \varepsilon_{tp}.|E_t|\right)\varepsilon_{tm} - \frac{\varepsilon_{tm}^2\cdot|E_t|}{2} - \frac{f_{tk}\cdot\varepsilon_{tp}}{2} - \frac{\varepsilon_{tp}^2\cdot|E_t|}{2}\right] \quad (17)$$

$$k_4 = 1 - \frac{-\frac{f_{tk}\cdot\varepsilon_{tp}^2}{6} + \left(\frac{f_{tk}}{2} + \frac{|E_t|\cdot\varepsilon_{tp}}{2}\right)\varepsilon_{tm}^2 - \frac{|E_t|\cdot\varepsilon_{tm}^3}{3} - \frac{\varepsilon_{tp}^3\cdot|E_t|}{6}}{\varepsilon_{tm}\left[\left(f_{tk}+\varepsilon_{tp}.|E_t|\right)\varepsilon_{tm} - \frac{\varepsilon_{tm}^2\cdot|E_t|}{2} - \frac{f_{tk}\cdot\varepsilon_{tp}}{2} - \frac{\varepsilon_{tp}^2\cdot|E_t|}{2}\right]} \quad (18)$$

In the case above, k_1 and k_2 are given by the same expressions presented earlier. In the following case, k_1 and k_2 are null.

6.3. For $\varepsilon_{tf} < \varepsilon_c \rightarrow \sigma_c = 0$

$$k_3 = \frac{1}{f_{tk}\,\varepsilon_{tm}}\left[\left(f_{tk} + \varepsilon_{tp}.|E_t|\right)\varepsilon_{tf} - \frac{\varepsilon_{tf}^2\cdot|E_t|}{2} - \frac{f_{tk}.\varepsilon_{tp}}{2} - \frac{\varepsilon_{tp}^2\cdot|E_t|}{2}\right] \quad (19)$$

$$k_4 = 1 - \frac{-\frac{1}{6}f_{tk}\cdot\varepsilon_{tp}^2 + \left(\frac{1}{2}f_{tk} + \frac{\varepsilon_{tp}.|E_t|}{2}\right)\frac{\varepsilon_{tf}^2}{3} - \frac{\varepsilon_{tf}^3\cdot|E_t|}{3} - |E_t|\frac{\varepsilon_{tp}^3}{6}}{\varepsilon_{tm}\left[\left(f_{tk}+\varepsilon_{tp}.|E_t|\right)\varepsilon_{tf} - \frac{\varepsilon_{tf}^2\cdot|E_t|}{2} - \frac{f_{tk}\cdot\varepsilon_{tp}}{2} - \frac{\varepsilon_{tp}^2\cdot|E_t|}{2}\right]} \quad (20)$$

Using these relations, the neutral axis equation is given by:

$$k_d = \frac{k_3.f_{tk}.H - \sum_{j=1}^{2}\sigma_{sj}.A_{sj}}{B_b(k_1.f_{ck} + k_3.f_{tk})} \quad (21)$$

In addition, the maximum deflection of the reinforced concrete beam is also obtained for a certain bending moment. For this case, Simpson formula was used based on the analytical expression for the bending moments in 1/2, 3/8, 1/4 and 1/8 of the span (BAZANT, 1984 [7]):

$$\delta = 2\int_0^{L/2} \frac{x}{2}.k(x)dx \cong \frac{L^2}{48}\left[k\left(\frac{L}{8}\right) + k\left(\frac{L}{4}\right) + 3k\left(\frac{3L}{8}\right) + k\left(\frac{L}{2}\right)\right] \quad (22)$$

7. AlfaMCV Software

Based on the equations presented in this work, a software was developed to model the behavior of a reinforced concrete beam, with rectangular section, simply supported with a point load centered in the middle of the span. The model presented and developed by the program seeks to simulate a real experimental test of a beam in a laboratory.

The AlfaMCV software is simple and versatile, developed using the programming language Visual Basic (2013). The software is in Portuguese. Fig.7.1. shows its main menu:

Fig. 7.1. AlfaMCV main screen (REIS, 2017 [[16]])

In the "Cálculos" (calculation) button, the user is referred to the window where he or she introduces all geometric characteristics of the section and materials (steel and concrete).

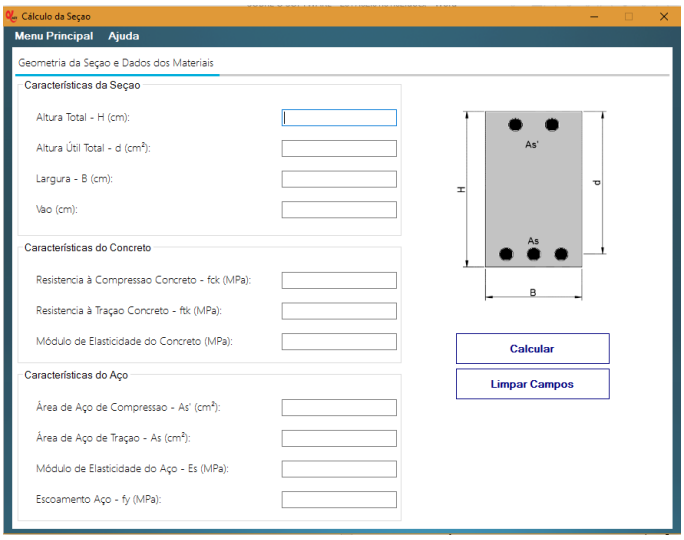

Fig. 7.2. Geometric data screen (REIS, 2017 [[16])

Based on the input data, the program calculates the behavior of the beam, presenting in a table characteristics such as the strain stage that the section is subjected to, neutral axis height, concrete and steel strains, bending moment and deflection in the beam, according to Fig.7.3.

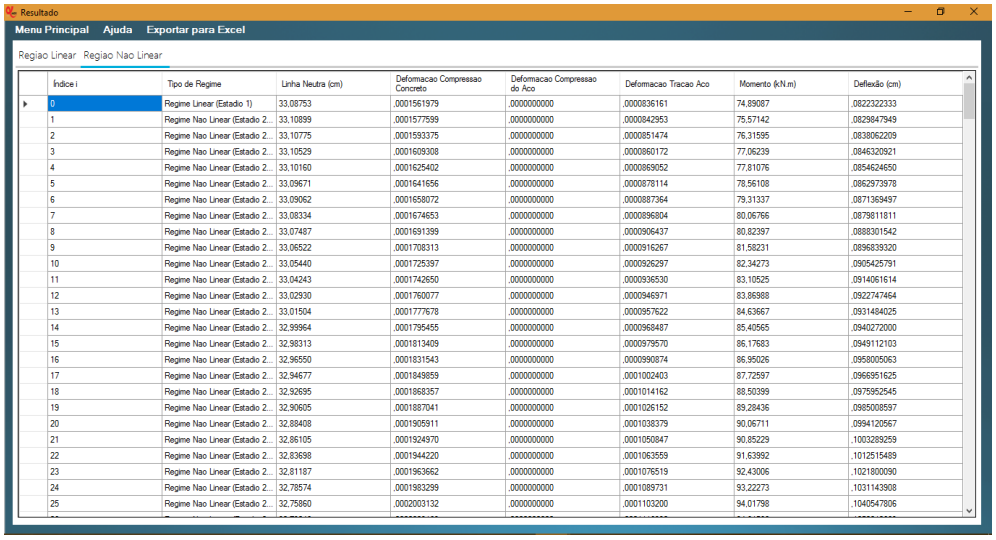

Índice i	Tipo de Regime	Linha Neutra (cm)	Deformacao Compressao Concreto	Deformacao Compressao do Aco	Deformacao Tracao Aco	Momento (kN.m)	Deflexão (cm)
0	Regime Linear (Estadio 1)	33,08753	,0001561979	,0000000000	,0000836161	74,89087	,0822322333
1	Regime Nao Linear (Estadio 2...	33,10899	,0001577599	,0000000000	,0000842953	75,57142	,0829847949
2	Regime Nao Linear (Estadio 2...	33,10775	,0001593375	,0000000000	,0000851474	76,31595	,0838062209
3	Regime Nao Linear (Estadio 2...	33,10529	,0001609308	,0000000000	,0000860172	77,06239	,0846320921
4	Regime Nao Linear (Estadio 2...	33,10160	,0001625402	,0000000000	,0000869052	77,81076	,0854624650
5	Regime Nao Linear (Estadio 2...	33,09671	,0001641656	,0000000000	,0000878114	78,56108	,0862973978
6	Regime Nao Linear (Estadio 2...	33,09062	,0001658072	,0000000000	,0000887364	79,31337	,0871369497
7	Regime Nao Linear (Estadio 2...	33,08334	,0001674653	,0000000000	,0000896804	80,06766	,0879811811
8	Regime Nao Linear (Estadio 2...	33,07487	,0001691399	,0000000000	,0000906437	80,82397	,0888301542
9	Regime Nao Linear (Estadio 2...	33,06522	,0001708313	,0000000000	,0000916267	81,58231	,0896839320
10	Regime Nao Linear (Estadio 2...	33,05440	,0001725397	,0000000000	,0000926297	82,34273	,0905425791
11	Regime Nao Linear (Estadio 2...	33,04243	,0001742650	,0000000000	,0000936530	83,10525	,0914061614
12	Regime Nao Linear (Estadio 2...	33,02930	,0001760077	,0000000000	,0000946971	83,86988	,0922747464
13	Regime Nao Linear (Estadio 2...	33,01504	,0001777678	,0000000000	,0000957622	84,63667	,0931484025
14	Regime Nao Linear (Estadio 2...	32,99964	,0001795455	,0000000000	,0000968487	85,40565	,0940272000
15	Regime Nao Linear (Estadio 2...	32,98313	,0001813409	,0000000000	,0000979570	86,17683	,0949112103
16	Regime Nao Linear (Estadio 2...	32,96550	,0001831543	,0000000000	,0000990874	86,95026	,0958005063
17	Regime Nao Linear (Estadio 2...	32,94677	,0001849859	,0000000000	,0001002403	87,72597	,0966951625
18	Regime Nao Linear (Estadio 2...	32,92695	,0001868357	,0000000000	,0001014162	88,50399	,0975952545
19	Regime Nao Linear (Estadio 2...	32,90605	,0001887041	,0000000000	,0001026152	89,28436	,0985008597
20	Regime Nao Linear (Estadio 2...	32,88408	,0001905911	,0000000000	,0001038379	90,06711	,0994120567
21	Regime Nao Linear (Estadio 2...	32,86105	,0001924970	,0000000000	,0001050847	90,85229	,1003289259
22	Regime Nao Linear (Estadio 2...	32,83698	,0001944220	,0000000000	,0001063559	91,63992	,1012515489
23	Regime Nao Linear (Estadio 2...	32,81187	,0001963662	,0000000000	,0001076519	92,43006	,1021800090
24	Regime Nao Linear (Estadio 2...	32,78574	,0001983299	,0000000000	,0001089731	93,22273	,1031143908
25	Regime Nao Linear (Estadio 2...	32,75860	,0002003132	,0000000000	,0001103200	94,01798	,1040547806

Fig. 7.3. Results screen (REIS, 2017 [[16])

It is worth mentioning that the software is able to export the generated table to an Excel™ worksheet, provided that the user possesses such a program installed on his/her computer.

In addition, the program is provided with a "Help" tab for the user, presenting a brief description of the software (also in Portuguese).

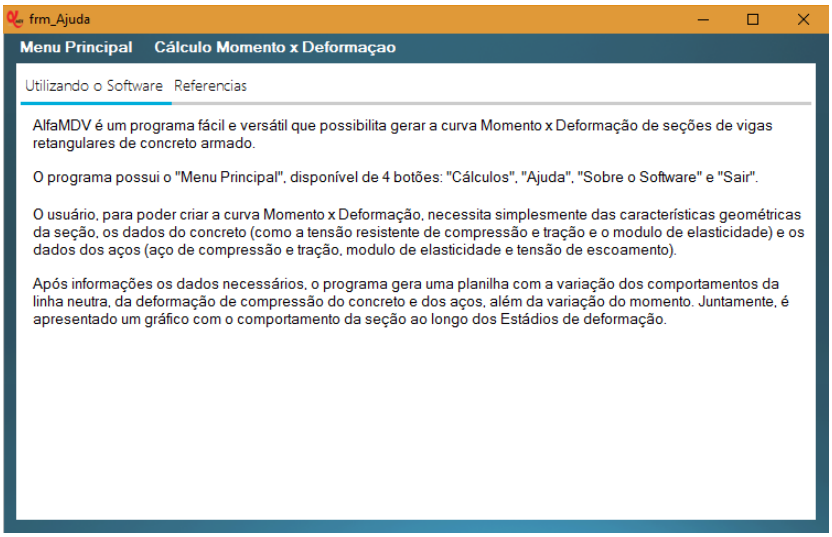

Fig. 7.4. Help screen (REIS, 2017 [[16]])

Finally, the "Sobre o Software" (About the Software) button on the main menu presents information about the institution (UERJ), its developer and advisors.

Fig.7.5. "About" screen (REIS, 2017 [[16]])

The software AlfaMCV is available for download at the following link: http://www.labbas.eng.uerj.br/pgeciv/nova/index.php?menu=downloads

8. Examples

For the validation of the software, analyses of under-reinforced, balanced, over-reinforced and doubly reinforced beams are carried out. Results were compared with the behavior of beams

for which the tensile strength is disregarded, as usually done by standards like NBR6118 (REIS, 2017 [[16]]).

The beams presented below are analyzed in the AlfaMCV software, for the cases where the tensile contribution is considered ($f_{tk} \neq 0$) and not ($f_{tk} = 0$) (REIS, 2017 [[16]]).

In all the analyses carried out, parameters for materials and geometry are given in Tab. 8.1. (REIS, 2017 [[16]]). Reinforcement was obtained by using the following formulae.

$$A_s = \omega \frac{d \,.b\,.\, f_{ck}}{f_{yk}} \tag{23}$$

$$\mu = \frac{M_k}{b \,.d^2 \,.f_{ck}} \tag{24}$$

To compare the obtained results for the beam deflection, the verification is performed while the beam is still in the elastic region. This analytical deflection is given for a simply supported beam submitted to a load *P* applied at the midpoint of the span *L*:

$$\delta = \frac{1}{48}\frac{Pl^3}{EI},\ I = \frac{bh^3}{12} \tag{25}$$

Parameter	Value
Beam height (h)	60 cm
Tensile reinforcement height (d)	55 cm
Width (b)	25 cm
Span (L)	200 cm
Concrete compressive strength (f_{ck})	30 MPa
Concrete tensile strength[1] (f_{tk})	2,8964 MPa
Concrete Elastic Modulus[2] (E_c)	27.605,21 MPa
Steel tensile/compressive strength (f_y)	500 MPa
Steel Elastic Modulus (E_y)	200.000 MPa

Tab. 8.1. Parameters used in examples (REIS, 2017 [[16]])

8.1.Under – Reinforced Beam

For this case, a reinforcement rate of ω = 0.015 was used (below the standard minimum value) and the resisting moment was obtained by NBR 6118 [[10]. Fig.8.1. shows the curves obtained by the software.

$A_s = 1{,}2375\ cm^2$

$M_k = 31{,}7625\ kN.m$

[1] The tensile strength is determined by NBR 6118:2014 [10], item 8.2.5

[2] The Elastic Module is determined by NBR 6118:2014 [10], item 8.2.8

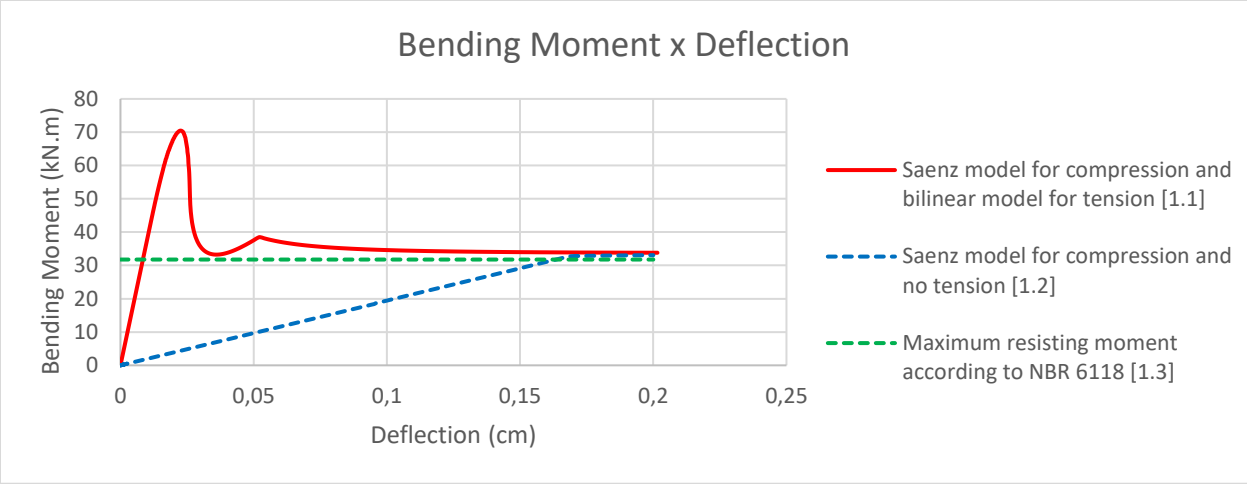

Fig. 8.1. Bending moment vs. deflection of under reinforced beam example

The red curve corresponds to the behavior of the reinforced concrete beam, with the parameters for geometry and material presented in Tab.8.1., with the consideration of the compression diagram of the concrete presented by SAENZ (1964) [[17], in addition to the tensile contribution presented by BAZANT (1984) [8].

The blue dotted curve presents the behavior of the same beam with the compression stresses given by SAENZ (1964) [[17], but with tensile stresses of the concrete equal to zero.

The limit given by the dotted green line presents the value based on equations given by Standard NBR6118 [[10], i. e., using the parabola-rectangle diagram in the compressive stresses of the concrete and disregarding tensile stresses. In these cases no safety factor is used.

For this type of beam, the red curve shows a considerable increase of the resistant moment and then a decay to approximately 33 kN.m, which corresponds to the bending moment given by the standard design code. This discrepancy is obviously due to the contribution of the tensile strength in concrete. For the final strain, in both cases the tensile region of concrete is fully cracked and the curves give the same bending moment.

Finally, the deflection of the beam is presented in order to compare the analytically obtained value with the one given by the program. Based on Equation (25), a 0.0118 cm deflection is obtained, while the software gave 0.01171 cm. This gives an error of 0.768%.

8.2.BALANCED BEAM

For this case, a reinforcement rate of ω = 0.178 was used (below the standard minimum value) and the resisting moment was obtained by NBR 6118 [[10]:

$A_s = 14{,}685\ cm^2$

$M_k = 360{,}73\ kN.m$

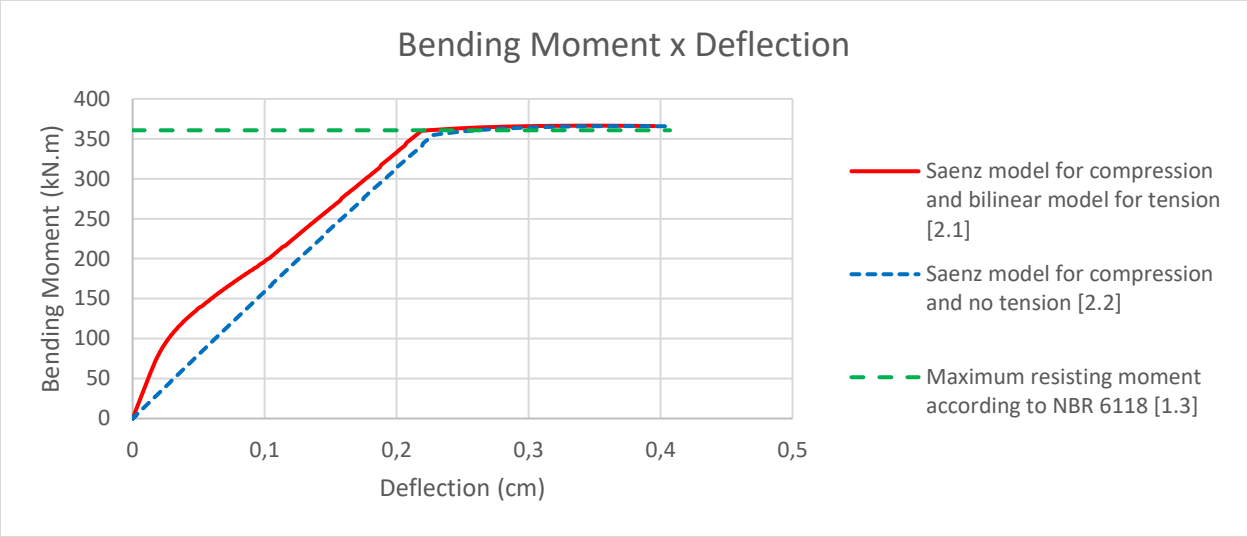

Fig. 8.2. Bending moment vs. deflection of balanced beam example

In this graph, the red and blue curves are closer when compared to the under-reinforced beam. This behavior is due to the greater contribution of the steel reinforcement in tension.

For the determination of the beam deflection, the standard equation gives a result of 0.01402 cm, while the program provides 0.012339 cm, error of 14.55%. This is mostly due to the stiffness provided by the steel that is not taken into account by NBR 6118 [[10].

8.3.Over – Reinforced Beam

For this case, a reinforcement rate of ω = 0.433 was used (below the standard minimum value) and the resisting moment was obtained by NBR 6118 [[10]:

$A_s = 35{,}72\ cm^2$

$M_k = 723{,}73\ kN.m$

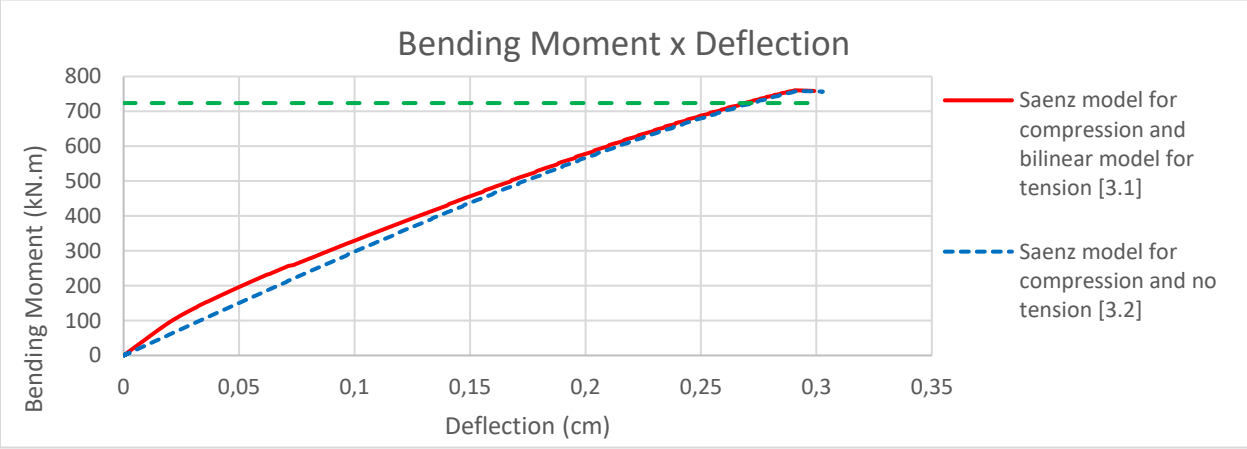

Fig. 8.3. Bending moment vs. deflection of over reinforced beam example

In this example, it is noted for the red and blue curves that there is no observable zero slope region, which indicates a sudden failure. The steel provided in the beam is such that concrete reaches the limiting values of strain prior to steel. This results in breaking of concrete and since now there is no concrete present to take the compression the beam fails suddenly.

For the determination of the beam deflection, the standard equation gives a result of 0.01734 cm, while the program provides 0.01328 cm, error of 30.58%. This is mostly due to the stiffness provided by the steel that is not taken into account by NBR 6118 [[10].

8.4.Doubly Reinforced Beam

For this particular case, the design of the reinforcement is based on a requesting bending moment. Thus, the following reinforcements are determined:

$A_{st} = 46{,}66\ cm^2$
$A_{sc} = 16{,}74\ cm^2$

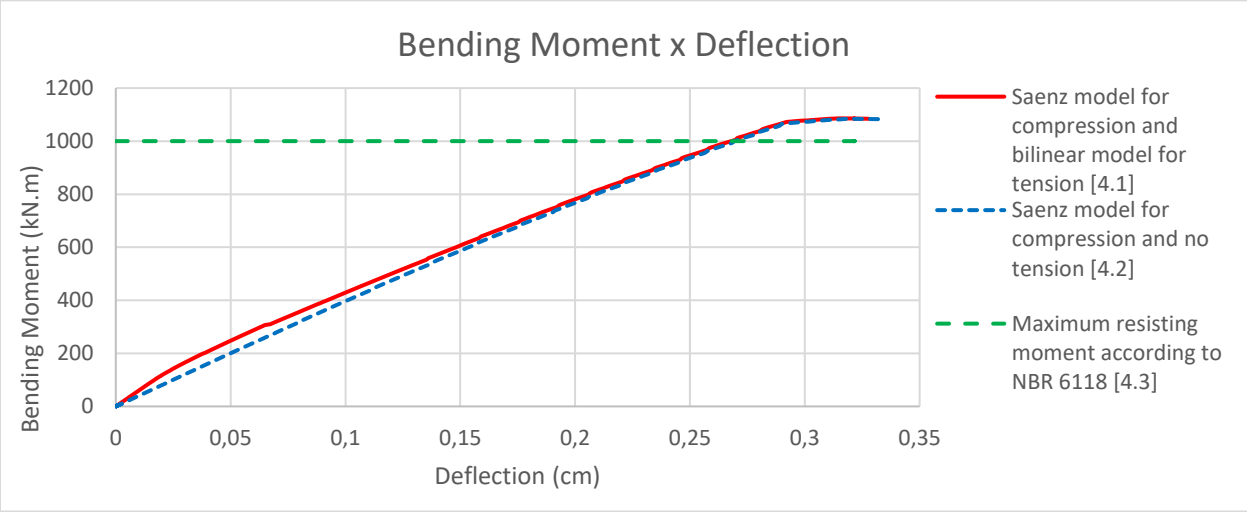

Fig. 8.4. Bending moment vs. deflection of doubly reinforced beam example

It is observed in this case that doubly reinforced beams behave very similar to the over-reinforced beams. The red and blue curves are considerably closer, due to the inefficient use of the tensile steel, reducing the contribution of concrete under tension.

For the determination of the beam deflection, the standard equation gives a result of 0.02059 cm, while the program provides 0.0128 cm, error of 60.86%. This is mostly due to the stiffness provided by the steel that is not taken into account by NBR 6118 [[10]. In this case, the contribution of the steel reinforcement is greater than previous examples.

9. Conclusions

This work aimed to present the developed software, AlfaMCV, which analyses reinforced concrete beams based on the models presented by SAENZ (1964) [17] for concrete compression and BAZANT (1984) [9] for concrete traction.

To prove the accuracy of the software, 4 case studies were carried out, in which the design of the beams was performed according to the pre-defined reinforcement rate or a required resisting moment.

Based on the results obtained in Fig.8.1. to 8.4., as the reinforcement rate increases, the curves that take into consideration the concrete under tension and the ones that only consider the concrete under compression tend to become closer. This behavior is justified since there are lower stresses in steel in tension (small strains) and higher stresses in concrete under compression. Such requests cause an increase in the formation of cracks and their propagation, raising the height of the neutral line. Finally, the tensile concrete has little influence on the collaboration during the increase of the bending moment in the beam, that is, between the moment of first cracking and the moment of rupture. Consequently, the bending moments for models considering the collaboration of the tension region of the concrete in comparison with models disregarding such contribution, become close.

Regarding the deflection, the software presented in this work is able to calculate its variation until failure. However, for practical purposes, the deflection found by the analytical theory and the program were compared, both for the elastic situation of the most requested section. In all cases studied, the higher the reinforcement rate of the section, the greater the discrepancy between the deflection obtained by the software and the one analytically calculated. This is justified by the fact that the standard NBR 6118 [10] considers only the geometry of the beam section, without the contribution of the steel in the stiffness, while the software considers the bending moment generated by the various sections of the structure, which depends on the equilibrium of the section, which is directly dependent characteristics of the constituent materials. In this way, larger stresses, such as larger areas of tensile steel and, if possibly, compression steel, in addition to the collaboration of both tension and compression of concrete along the curves, generate smaller deflections in the beam.

REFERENCES

[10] ASSOCIAÇÃO BRASILEIRA DE NORMAS TÉCNICAS. *NBR 6118: Projeto de estruturas de concreto - Procedimento*. Rio de Janeiro, 2014.

[11] BAZANT, Z. P., OH, B. H. *Deformation of Progressively Cracking Reinforced Concrete Beams*. ACI JOURNAL, 1984. Vol 81, n° 3.

[12] BAZANT, Z. P. *Fracture in Concrete and Reinforced Concrete*. Ed. John Wiley & Sons Ltd, 1985.

[13] BAZANT, Z.P, MARCHERTAS, A. H., PFEIFFER, P. A. *Blunt – Crack Band Propagation in Finite – Element Analysis for Concrete Structures*. 7th International Conference on SMIRT, Chicago. 1983.

[14] PFEIL, W. *Concreto Armado Dimensionamento*. Ed AO LIVRO TÉCNICO S.A., 1969. Rio de Janeiro – RJ.

[15] PROENÇA, S. P. B., *Sobre Modelos Matemáticos do Comportamento não-linear do Concreto: Análise Crítica e Contribuições*. Universidade de São Carlos, SP, 1988.

[16] REIS, A. W. de Q. R., *Modelagem Numérica de Seções de Concreto Armado***.** Universidade do Estado do Rio de Janeiro. Rio de Janeiro – RJ, 2017.

[17] SCANLON, L. P. *Discussion of "Equation for the Stress – Strain Curve of Concrete"* by Prakash Desayi and S. Krishnan, ACI Journal, *Proceedings* V.61, N°9, Set, 1964, pp. 1229-1235.

[18] SCANLON, A. *Time – Dependent Deflections of Reinforced Concrete Slabs*. PhD. Thesis, Alberta University, Edmonton, 1971.

[19] VITTORIO, S. de. *Time – Dependent Behaviour of Reinforced Concrete Slabs*. Università di Bologna, 2011.

REQUIRED METADATA

Current code version

Nr	Code metadata description	*Please fill in this column*
C1	Current code version	*Version 1.1*
C2	Permanent link to code/repository used of this code version	*http://www.labbas.eng.uerj.br/pgeciv/nova/files/AlfaMCV_sib.exe*
C3	Legal Code License	*BR5120160014342*
C4	Code versioning system used	*none*
C5	Software code languages, tools, and services used	*Visual Basic*
C6	Compilation requirements, operating environments & dependencies	Microsoft Windows .NET Framework 4.5
C7	If available Link to developer documentation/manual	*none*
C8	Support email for questions	*anawaldila@hotmail.com* *rburgos@eng.uerj.br* *margareth.magalhaes@uerj.br*

Tab. 1. Code metadata